Centralized Traffic Control via Small Fleets of Connected and Automated Vehicles

Chiara Daini, Paola Goatin, Maria Laura Delle Monache, Antonella Ferrara

Centralized Traffic Control via Small Fleets of Connected and Automated Vehicles

Chiara Daini[1], Paola Goatin[2], Maria Laura Delle Monache[3] and Antonella Ferrara[4]

***Abstract*— In this paper we propose a model for mixed traffic composed of few Connected and Automated Vehicles (CAVs) in the bulk flow. We rely on a multi-scale approach, coupling a Partial Differential Equation describing the overall traffic flow and Ordinary Differential Equations accounting for CAV trajectories, which act as moving bottlenecks on the surrounding flux. In our framework, CAVs are allowed to overtake (if on different lanes) or merge (if on the same lane). Controlling CAV desired speeds allows to act on the system to minimize any traffic density dependent cost function. More precisely, we apply Model Predictive Control to reduce fuel consumption in congested situations. In particular, we observe how the CAV number impacts the result, showing that low penetration rates are sufficient to significantly improve the selected performance indexes. The outcome of this paper supports the attractive perspective of exploiting a small number of controlled vehicles as endogenous actuators to regulate traffic flow on road networks.**

I. INTRODUCTION

New technologies are impacting how we operate, control and manage traffic. More specifically, the adoption of more technologically sophisticated vehicles might revolutionize the way in which we look at traffic. Connected and automated vehicles (CAVs) are expected to dominate the market of vehicles in the next future, so it is fundamental that we understand how they interact with the overall traffic and how they can be leveraged to improve traffic conditions and safety.

In the past few years, several researchers started looking at how CAVs would impact traffic flow and how it is possible to use them to control the human-driven counter-part to mitigate congestion and improve throughput. In particular, studies focused on understanding the impact of CAVs on traffic emissions both from a theoretical point of view [1]–[6], and from an experimental side [7].

The field experiment described in [7] showed that even a small percentage of automated vehicles among the traffic can bring benefits to the whole system, by dissipating stop-and-go waves, improving the throughput and reducing traffic flow emissions and consumption.

*This work was supported by ERASMUS+/KA1 "NORTH SOUTH TRAINEESHIP" academic year 2020/21

[1] Chiara Daini is with Inria Paris, Kopernic Research Group, Paris, France chiara.daini@inria.fr

[2]Paola Goatin is with Université Côte d'Azur, Inria, CNRS, LJAD, France paola.goatin@inria.fr

[3]Maria Laura Delle Monache is with the Department of Civil and Environmental Engineering, University of California, Berkeley, USA mldellemonache@berkeley.edu

[4]Antonella Ferrara is with Department of Electrical, Computer and Biomedical Engineering, University of Pavia, Pavia, Italy antonella.ferrara@unipv.it

From the modeling and control points of view, the idea of using vehicles as moving actuators in the form of moving bottlenecks was introduced in [6], [8] and [1]. In [6], the authors use a single vehicle as a control actuator for the overall traffic, implementing a Model Predictive Control (MPC) strategy to reduce the global fuel consumption of vehicles. The authors show a reduction in traffic flow emissions related to a reduction in congestion caused by a fixed bottleneck located downstream. In [1] and [2], a CTM approach is applied to use CAVs as traffic control actuators. The CAV changes its speed according to a specific control that allows to reduce the overall traffic congestion and the average travel time. This idea was then expanded by the same authors to include truck platoon merging in [3] and several vehicles in [4], [5]. All of these works focus on improving the energy footprint of traffic by either dissipating stop-and-go waves or reducing traffic congestion. In [4], the authors create specific moving bottlenecks to reduce the congestion and to allow traffic at free flow in the fixed bottleneck, while in [5] the same concept is exploited by using truck platooning. A similar goal is tackled by [9] using a different approach based on a data-driven cruise control in a microscopic framework. We remark than none of these works include overtaking situations among the controlled moving bottlenecks.

In this paper, the CAVs are distributed on several lanes and they are allowed both to merge and to overtake. This is a step forward with respect to the current state of the art about traffic flow optimization strategies based on controlled CAVs. To our knowledge, moving bottleneck overtaking was introduced only in [10], through a different modeling framework and for different optimization purposes. The proposed model, apart from being useful to design the optimization-based control exploiting the small fleet of CAVs, is also useful to develop a simulation environment to model general interactions among CAVs and the overall traffic, and which enable to use CAVs as control actuators with the goal or reducing the overall traffic emissions.

The paper is organized as follows: Section II details the model framework, providing a mathematical description of the fully coupled PDE-ODE model and the interactions among CAVs. Section III illustrates the control framework and the MPC algorithm, while Section IV describes the numerical scheme and shows the results of the numerical experiments.

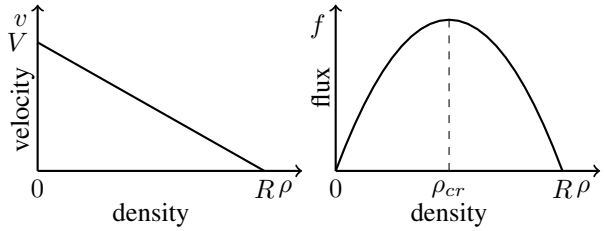

Fig. 1: Quadratic fundamental diagram.

II. DESCRIPTION OF THE MATHEMATICAL MODEL

The mathematical model used in the present investigation is the classical Lighthill-Whitham-Richards (LWR) equation [11], [12], a *macroscopic first-order* model based on the principle of conservation of the number of cars and on a phenomenological closure relation between traffic density and mean velocity. Macroscopic models, also called *hydrodynamic* models, describe the traffic flow as a fluid, reproducing the spatio-temporal evolution of aggregated quantities. The macroscopic quantities involved in the model are the following:

- the traffic density $\rho = \rho(t, x)$, defined as the number of vehicles per unit length of the road (veh/km);
- the flow $f = f(t, x)$, defined as the number of vehicles passing the cross-section at location x per unit time (veh/h);
- the mean speed $v = v(t, x)$, which is the arithmetic mean speed of the vehicles passing the cross-section per unit time (km/h).

The above quantities are linked by the hydrodynamic flow relation $f = \rho v$. Assuming $v = v(\rho)$, the scalar conservation law expressing the mass conservation reads

$$\frac{\partial \rho}{\partial t} + \frac{\partial f(\rho)}{\partial x} = 0, \tag{1}$$

where the *fundamental diagram* $f = f(\rho) = \rho v(\rho)$ expresses the flux as a function of the density. In the last decades, several studies have been carried out and different fundamental diagrams have been proposed to describe the real world traffic in the most accurate way, see e.g. [13], [14]. In this paper, we consider the model proposed by Greenshields [15] that assumes a linear decreasing dependence of the speed on the traffic density

$$v(\rho) = V\left(1 - \frac{\rho}{R}\right), \tag{2}$$

where V denotes the maximal speed and R the maximal (bump-to-bump) density on the road. As a result, the fundamental diagram is a quadratic function (see Fig. 1)

$$f(\rho) = V\rho\left(1 - \frac{\rho}{R}\right), \tag{3}$$

attaining its maximum at $\rho_{cr} = R/2$. We note that our approach could be extended to any fundamental diagram $f : [0, R] \to \mathbb{R}_+$ with $f(0) = f(R) = 0$, which is concave in the free-flow interval $[0, R/2]$.

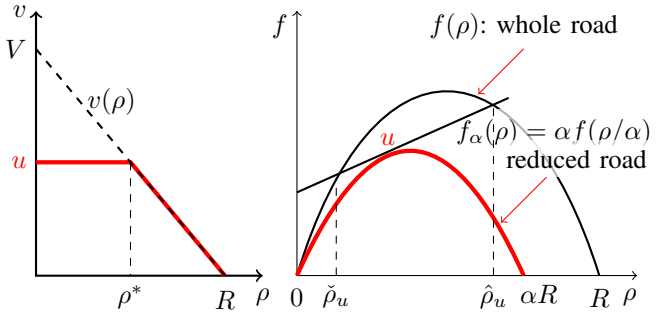

Fig. 2: Left: CAV speed depending on downstream traffic density. Right: reduced flow at CAV position.

The presence of slow moving vehicles and their interactions with bulk traffic, has been studied by several authors, see e.g. [1], [16]–[20]. Here we extend the model proposed in [21] and then developed in [22], [23], which consists in the LWR equation describing the general evolution of the traffic density and an Ordinary Differential Equation (ODE) which takes into account the CAV trajectory. The fully coupled PDE-ODE model including several CAVs writes:

$$\frac{\partial}{\partial t}\rho\,(t,x) + \frac{\partial}{\partial x} f\,(\rho\,(t,x)) = 0, \tag{4a}$$

$$\rho(0,x) = \rho_0(x), \tag{4b}$$

$$f(\rho(t,0)) = f_{in}(t), \tag{4c}$$

$$f(\rho(t,L)) = f_{out}(t), \tag{4d}$$

$$f\,(\rho\,(t, y_\ell(t))) - \dot{y}_\ell(t)\rho\,(t, y_\ell(t)) \le \frac{\alpha R}{4V}(V - \dot{y}_\ell(t))^2, \tag{4e}$$

$$\dot{y}_\ell(t) = \min\{u_\ell(t), v(\rho(t, y_\ell(t)+))\}, \tag{4f}$$

$$y_\ell(0) = y_\ell^0. \tag{4g}$$

In (4), $x \in [0, L]$, $L > 0$ being the length of the road stretch considered, $t \in [0, T_f]$ the time interval and ρ_0 the initial traffic density. The time-dependent variables $y_\ell = y_\ell(t)$, $\ell = 1, \dots, N$, represent the N CAV positions, whose desired speeds are the controlled time dependent variables $u_\ell : [0, T_f] \to [0, V]$, $\ell = 1, \dots, N$. Each moving bottleneck therefore moves at its maximal speed until the downstream traffic density $\rho(t, y_\ell(t)+)$ allows it, and it adapts to the surrounding traffic velocity when the average speed decreases (Fig. 2, left). In particular, CAVs cannot change lane to overtake the cars, but can overtake each other if they belong to different lanes. Moreover, each automated vehicle acts as a moving capacity constraint and this is expressed by the relation (4e), where $\alpha \in]0, 1[$ is the reduction rate of the road capacity due to the presence of the vehicle itself, here set to $\alpha = (M-1)/M$, where $M \in \mathbb{N}$ denotes the number of lanes. When active, the constraint induces the formation of a non-classical discontinuity in the traffic density, moving with speed $u_\ell(t)$ with upstream density value $\hat{\rho}_{u_\ell(t)}$ and downstream density $\check{\rho}_{u_\ell(t)}$ (see Fig. 2, right).
Our modeling framework allows to take into account interactions between the automated vehicles, that happen when

$y_i(\bar{t}) = y_j(\bar{t})$, for some $i, j = 1, \dots, N$, $i \neq j$ and $\bar{t} \in [0, T_f]$. For simplicity, we assume that each vehicle can occupy only one lane and we do not allow lane changing. We can therefore have two types of interactions, depending if the vehicles share the **same lane** or are on **different lanes**:

- If the vehicles are on the same lane, the upstream vehicle travelling with higher speed will adapt to the preceding vehicle and follow it: we get $y_i(t) = y_j(t)$ and $u_i(t) = u_j(t)$ for $t \geq \bar{t}$.
- If the vehicles are on different lanes, the faster simply overtakes the slower.

Besides, the constraints (4e) continue to act after the interaction, see Fig. 3.

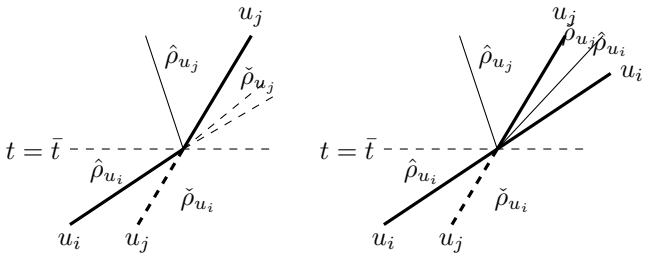

Fig. 3: Examples of interacting CAV trajectories (bold lines). Left: same lane. Right: different lanes.

III. CENTRALIZED CONTROL OF FLEETS

In order to optimize the entire traffic, considering a selected functional, we design a centralized control of a fleet of N CAVs. The aim is to compute an "optimal control" $u^* = (u_1^*, \dots, u_N^*) : [0, T_f] \to \mathbb{R}^N$ minimizing a chosen performance index (the *cost function*). Aiming at reducing fuel consumption and the associated pollutant emissions in case of traffic congestion, we concentrate here on the Total Fuel Consumption (TFC) introduced in [8] and later considered in [6], [24], which is defined as $TFC(\rho) = \rho FC(\rho)$, where, due to the first order modeling setting not accounting for accelerations, it is assumed that the fuel consumption rate $FC(\rho) = K(v(\rho))$ is described as a function of the traffic density through its relation to the average traffic speed. This dependence relation is approximated by a sixth order polynomial $K(v)$, that expresses the fuel consumption as a function of the speed:

$$\begin{aligned} K(v) = {} & 5.7 \cdot 10^{-12} \cdot v^6 - 3.6 \cdot 10^{-9} \cdot v^5 \\ & + 7.6 \cdot 10^{-7} \cdot v^4 - 6.1 \cdot 10^{-5} \cdot v^3 \\ & + 1.9 \cdot 10^{-3} \cdot v^2 + 1.6 \cdot 10^{-2} \cdot v + 0.99. \end{aligned} \tag{5}$$

Above, $K(v)$ is expressed in [Liters/hr] and v in [km/hr].

A Model Predictive Control (MPC) approach has been selected, since it can deal with nonlinear systems, multi-criteria optimization and constraints [25]. The MPC is a method of process control that computes the optimal value of the defined control variable based on the selected functional cost over a predicted evolution of the system. The mentioned predicted evolution is obtained through an optimisation algorithm requiring, at each iteration step, a simulation of the system (4). The control acts on the values of the fleet vehicle speeds, modifying it according to the prediction. At the k-th iteration step, we compute the optimal (constant) speed value $u_\ell^*(k)$ for each CAV, taking the current density value $\rho(t_k, \cdot)$ as the initial datum in (4) over a fixed time horizon $[t_k, t_k + \Delta T]$, with $\Delta T = 15$ min:

$$u^*(k) = \arg\min \left\{ \int_{t_k}^{t_k + \Delta T} \int_0^L TFC(\rho(t,x)) dx dt \right\}, \tag{6}$$

subject to (4) and to the constraints

$$u_{\min} \leq u_\ell \leq u_{\max}, \quad \ell = 1, \dots, N. \tag{7}$$

The problem is solved via a receding horizon approach. The optimization horizon is set to 15 minutes and the computation step, in which the optimal control is applied, is set to 5 minutes. This means that at any iteration the optimal speed vector $u^*(k)$ is computed on the time interval $[t_k, t_k + \Delta T]$, with $\Delta T = 15$ min, and then applied to the controlled vehicles for the time interval $[t_k, t_k + \Delta\tau]$, with $\Delta\tau = 5$ min and the traffic density and CAV's positions at time $t_{k+1} = t_k + \Delta\tau$ are used to initialize the next iteration step. We refer to Algorithm 1 for an overview of the procedure. The optimization problems have been solved using the MATLAB function `fmincon`, a gradient-based method that is designed for non-linear constrained problems, initialized with the optimal velocities computed by `bayesOpt`, a Bayesian optimizer which uses a Gaussian process model to minimize the objective function, thus better exploring the admissible control domain, to avoid local minima.

Algorithm 1 MPC algorithm

Data: Input initial traffic density ρ_0, CAV positions y_ℓ^0 and velocities $u_\ell(0)$, time horizon T_f, optimization time interval ΔT, simulation time interval $\Delta\tau$
Result: CAV optimal velocities $u_\ell^*(k)$
while $t_k \leq T_f$ **do**
  for $t \in [t_k, t_k + \Delta T[$ **do**
    Solve (6) - (4) for optimal solutions $u_\ell^*(k)$
  end
  for $t \in [t_k + t_k + \Delta\tau[$ **do**
    Apply (4) with the optimal solution $u_\ell \leftarrow u_\ell^*(k)$
  end
  $t_k \leftarrow t_k + \Delta\tau$ and update the traffic variables $\rho(t_k)$, $y_\ell(t_k)$ and $u_\ell(t_k)$
end

The practical implementation requires the knowledge of the traffic density distribution and the CAV positions and velocities on the considered road stretch at each iteration time t_k, as well as (a prediction of) the inflow $f_{in}(t)$ and outflow $f_{out}(t)$ for $t \in [t_k, t_k + \Delta T]$.

IV. NUMERICAL SIMULATIONS

A. Numerical scheme

We briefly describe the approximation method used to solve the coupled PDE-ODE model (4). The scheme is

composed of two parts: first, we discretize the PDE (4a) with the constraint (4e) and then we solve numerically the ODEs (4f).

1) Numerical scheme for PDE (4a) *with constraint:* To approximate the LWR model, we use the reconstruction scheme introduced in [26]. It uses a conservative finite volume scheme for the constrained hyperbolic PDE using a flux reconstruction technique at the constraint locations. Let Δx and Δt be the fixed space and time steps satisfying the Courant-Friedrichs-Lewy (CFL) condition [27]:

$$V\Delta t = 0.9\,\Delta x,$$

and set $x_{j-1/2} = j\Delta x$, $x_j = (j+1/2)\Delta x$ for $j = 0, \dots, J$, with $x_{-1/2} = 0$, $x_{J+1/2} = L$, and $t^n = n\Delta t$ for $n \in \mathbb{N}$. The numerical scheme consists in the following steps:

- **Step 1.** Approximate the initial data ρ_0 with piece-wise constant functions $\rho_0^n = \{\rho_{0,j}^n\}_{j=0}^J$.
- **Step 2.** Locate the cell position C_{m_ℓ} of the ℓ-th CAV at time t^n, $\ell = 1, \dots, N$.
- **Step 3.** Compute the Godunov numerical fluxes [28] at the cell interfaces $F_{j+\frac{1}{2}}^n = F(\rho_j^n, \rho_{j+1}^n)$, which in this case can be derived using the supply-demand formula

$$F(\rho_j^n, \rho_{j+1}^n) = \min\{D(\rho_j^n), S(\rho_{j+1}^n)\}, \qquad (8)$$

where

$$D(\rho) = f(\min\{\rho, \rho_{cr}\}), \quad S(\rho) = f(\max\{\rho, \rho_{cr}\})$$

(as in the Cell Transmission Model [29]).
- **Step 4.** For $\ell = 1, \dots, N$, if the constraint (4e) is not satisfied for the Riemann solution corresponding to $\rho_{m_\ell-1}^n$, $\rho_{m_\ell+1}^n$, then we assume a moving bottleneck at $\bar{x}_{m_\ell} = x_{m_\ell-1/2} + d_{m_\ell}^n \Delta x \in C_{m_\ell}$ with $d_{m_\ell}^n = \dfrac{\check{\rho}_{u_\ell^n} - \rho_{m_\ell}^n}{\check{\rho}_{u_\ell^n} - \hat{\rho}_{u_\ell^n}}$ and go to Step 5. Otherwise, if the constraint (4e) is satisfied, move directly to Step 6.
- **Step 5.** If $0 \le d_{m_\ell}^n \le 1$, then
  - Compute $\Delta t_{m_\ell}^n = \dfrac{1 - d_{m_\ell}^n}{u_\ell^n} \Delta x$.
  - Replace $F_{m_\ell-\frac{1}{2}}^n$ and $F_{m_\ell+\frac{1}{2}}^n$ by $F_{m_\ell-\frac{1}{2}}^n = F(\rho_{m_\ell-1}^n, \hat{\rho}_{u_\ell^n})$ and $\Delta t F_{m_\ell+\frac{1}{2}}^n = \min(\Delta t_{m_\ell}^n, \Delta t) f(\check{\rho}_{u_\ell^n}) + \max(\Delta t - \Delta t_{m_\ell}^n, 0) f(\hat{\rho}_{u_\ell^n})$.
- **Step 6.** For $j = 0, \dots, J$, update the density with the conservative formula

$$\rho_j^{n+1} = \rho_j^n - \frac{\Delta t}{\Delta x}\left(F_{j+\frac{1}{2}}^n - F_{j-\frac{1}{2}}^n\right), \qquad (9)$$

where the boundary numerical fluxes $F_{-\frac{1}{2}}^n$ and $F_{J+\frac{1}{2}}^n$ are computed setting $D(\rho_{-1}^n) = f_{in}(t^n)$ and $S(\rho_{J+1}^n) = f_{out}(t^n)$ in (8).

Above, we set $u_\ell^n = u_\ell(t^n)$. Remark that, when in the same cell, the moving bottlenecks are treated sequentially one after the other, first those which are not active (i.e. satisfy (4e)), then those which are active (violating (4e)).

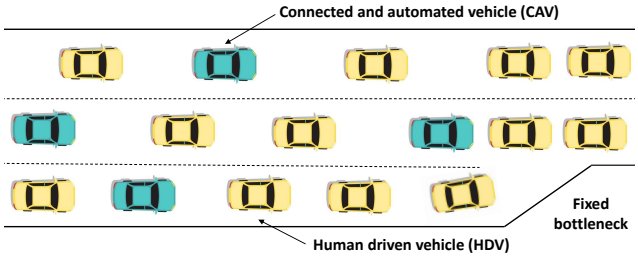

Fig. 4: Simulation framework

2) Numerical method for the ODE: To track the CAV trajectories, at each time step, we update the positions y_ℓ^n of the ℓ-th CAV using an explicit Euler scheme $y_\ell^{n+1} = v(\rho^n)\Delta t^n + y_\ell^n$ for $\ell = 1, \dots, N$.

B. Numerical results

We consider a section of highway of length $L = 50$ km with $M = 3$ lanes (we set $\alpha = 0.6$), uniform road conditions with no on- or off-ramps or other inhomogeneities (see Fig. 4). The maximum speed and maximum density have been chosen equal to, respectively, $V = 140$ km/h and $R = 400$ veh/km (considering 5 m of average vehicle length and its 50% of safety distance). As initial datum, we consider a constant density $\rho_0 = 0.3R$. The simulation time horizon T_f has been set equal to 1 hour.

The boundary conditions are given by the following inflow $f_{in}(t)$ and an outflow $f_{out}(t)$:

$$f_{in}(t) = \begin{cases} f_{max} & \text{if } t \le 0.5T_f, \\ 0 & \text{if } t > 0.5T_f, \end{cases} \qquad (10)$$

$$f_{out}(t) = 0.5\, f_{max} \quad \forall t \in [0, T_f], \qquad (11)$$

where we have set $f_{max} = \max_{\rho\in[0,R]} f(\rho) = f(R/2)$ the maximal flow on the road. Condition (11) mimics the presence of a fixed bottleneck at the end of the road, inducing a backward moving congestion whose effects we aim at reducing.

The tests have been performed on fleets of up to 10 vehicles, initially placed at fixed locations for each simulation. We initially assigned a velocity of 50 km/h to each CAV and we distributed them homogeneously on the road, such that $y_1^0 = 4,5$ km and $y_\ell^0 = y_{\ell-1}^0 + 4,5$ km. Moreover, CAVs were assigned sequentially to different lanes 1 to 3.

The cost functional TFC underwent two optimization procedures, one optimizing the CAV speeds on the whole time horizon of 1 hour and the other using the MPC strategy described in Section III, taking $u_{\min} = 30$ km/h, $u_{\max} = 100$ km/h as control bounds in (7). Fig. 5 shows the two trends: one can observe that the 1 hour optimization is regularly decreasing as the number of CAVs increases, and it seems to stabilize approaching to the maximum number of vehicle we considered. On the other hand, the MPC optimization is less effective and its trend is less stable, but it still shows a decreasing tendency with the increasing number of vehicles. This difference can be attributed to the different prediction horizons of the two optimizers.

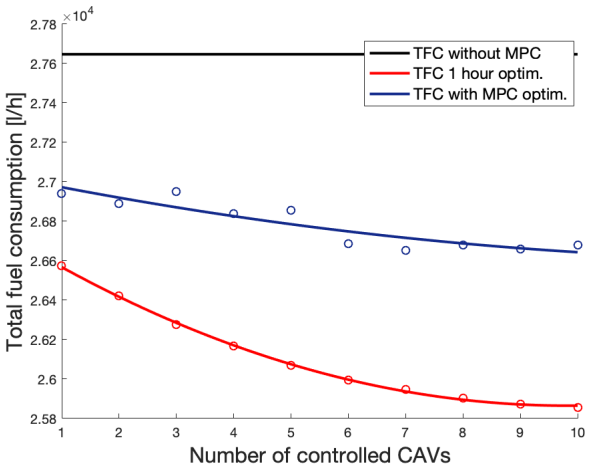

Fig. 5: TFC optimizations varying the CAV fleet sizes

Nevertheless, MPC uses a more realistic approach, updating traffic evolution every 5 min, and making predictions on a shorter time horizon.

	TFC 1 hour opt. [liters/h]	TFC reduction %
Uncontrolled	$2.7647 \cdot 10^4$	0
1 CAV	$2.6573 \cdot 10^4$	3.88
5 CAVs	$2.6071 \cdot 10^4$	5.70
10 CAVs	$2.5856 \cdot 10^4$	6.48

TABLE I: Comparison between total fuel consumption 1 hour optimization results for different CAV fleet sizes.

	TFC with MPC [liters/h]	TFC reduction %
Uncontrolled	$2.7647 \cdot 10^4$	0
1 CAV	$2.6941 \cdot 10^4$	2.56
5 CAVs	$2.6856 \cdot 10^4$	2.87
10 CAVs	$2.6680 \cdot 10^4$	3.49

TABLE II: Comparison between total fuel consumption MPC results for different CAV fleet sizes.

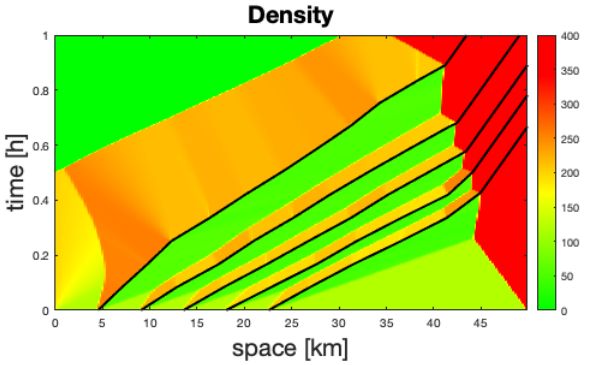

Fig. 6: Traffic density with MPC on a fleet of 5 CAVs

In Tables I and II, we show the percentage of fuel consumption reduction as the number of CAVs in the fleet

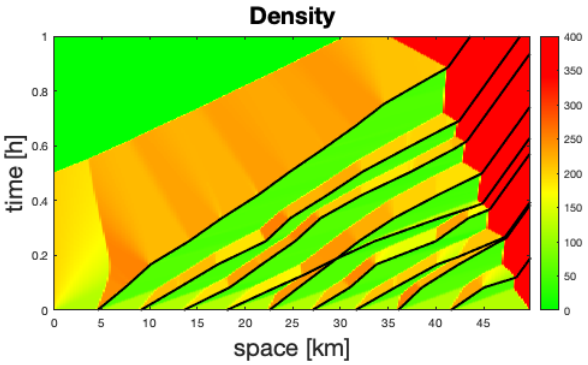

Fig. 7: Traffic density with MPC on a fleet of 9 CAVs

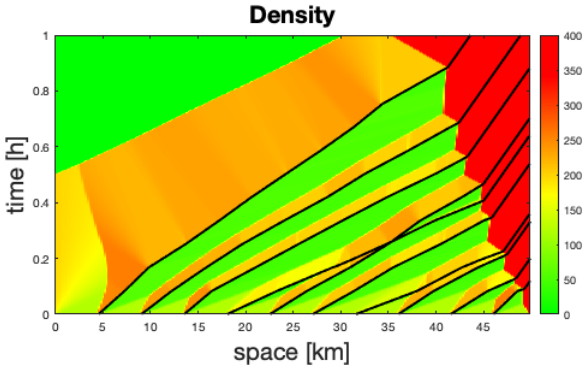

Fig. 8: Traffic density with MPC on a fleet of 10 CAVs

	1 CAV	5 CAVs	10 CAVs
Velocity [km/h]	53.55	52.89	51.97
		54.72	55.16
		54.63	56.77
		56.00	56.57
		56.85	55.82
			58.00
			51.82
			56.74
			52.81
			56.17

TABLE III: Optimal velocities for 1 hour optimisation with different CAV fleet sizes.

increases. Simulations evidence that a larger fleet leads to increased reduction of the functional cost analyzed, but the rate of improvement decreases as the number of CAVs increases. Table III and Fig. 9 show the optimal velocities applied to the CAVs for specific fleet sizes.

Figures 6, 7 and 8 show the optimal traffic density space-time evolution and the optimal CAV trajectories. We see that the red region, corresponding to the traffic jam caused by the bottleneck at the end of the road, is reduced by the CAV action. At the same time, moderate congestion can be observed upstream CAVs, due to the corresponding road capacity reduction. Once in congestion, CAVs are forced to slow down and adapt their velocity to the average one. In Figures 7 and 8, it is possible to see interactions of vehicles travelling on different lanes, where the faster overtakes the slower. In both cases, they are the 4th and the 5th CAVs,

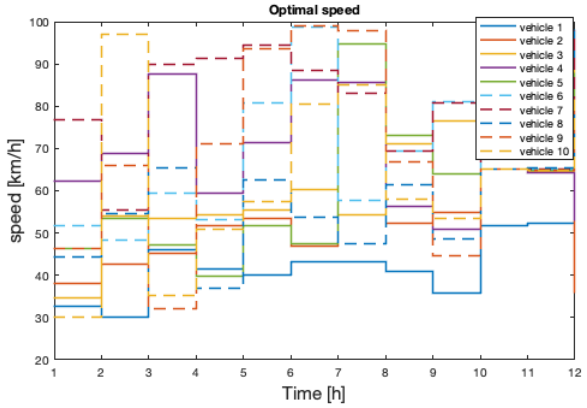

Fig. 9: Optimal control velocities computed by MPC on a fleet of 10 CAVs

respectively in lane 1 and lane 2.

V. CONCLUSIONS

In this paper, we investigated the advantages of mixed traffic solutions, where CAV fleets act in a consistent way on the fuel consumption of the entire flow and hence decrease the overall pollution produced by the overall traffic. The MPC is here acting as a centralized control on all the CAVs regarded as actuators. As future work, we plan to extend this approach to decentralized controls, which act on each controlled variable separately, and more realistic partially centralized methods, in which the controlled vehicles are able to detect other CAVs near them and to adapt their own velocities accordingly.

ACKNOWLEDGMENT

This work has been realized during C.D.'s Master internship at Inria Sophia Antipolis, France.

REFERENCES

[1] M. Čičić and K. H. Johansson, "Traffic regulation via individually controlled automated vehicles: a cell transmission model approach," in *2018 21st International Conference on Intelligent Transportation Systems (ITSC)*, 2018, pp. 766–771.

[2] ——, "Stop-and-go wave dissipation using accumulated controlled moving bottlenecks in multi-class CTM framework," in *2019 IEEE 58th Conference on Decision and Control (CDC)*, 2019, pp. 3146–3151.

[3] ——, "Energy-optimal platoon catch-up in moving bottleneck framework," in *2019 18th European Control Conference (ECC)*, 2019, pp. 3674–3679.

[4] M. Čičić, I. Mikolášek, and K. H. Johansson, "Front tracking transition system model with controlled moving bottlenecks and probabilistic traffic breakdowns," *IFAC-PapersOnLine*, vol. 53, no. 2, pp. 14 990–14 996, 2020, 21st IFAC World Congress. [Online]. Available: https://www.sciencedirect.com/science/article/pii/S2405896320326288

[5] M. Čičić, L. Jin, and K. H. Johansson, "Coordinating vehicle platoons for highway bottleneck decongestion and throughput improvement," 2020.

[6] G. Piacentini, P. Goatin, and A. Ferrara, "Traffic control via moving bottleneck of coordinated vehicles," *IFAC-PapersOnLine*, vol. 51, no. 9, pp. 13–18, 2018.

[7] R. E. Stern, S. Cui, M. L. D. Monache, R. Bhadani, M. Bunting, M. Churchill, N. Hamilton, R. Haulcy, H.Pohlmann, F. Wu, B. Piccoli, B. Seibold, J. Sprinkled, and D. Work, "Dissipation of stop-and-go waves via control of autonomous vehicles: Field experiments," *Transportation Research Board 96th Annual Meeting*, 2017.

[8] R. A. Ramadan and B. Seibold, "Traffic flow control and fuel consumption reduction via moving bottlenecks," 2017, preprint, https://arxiv.org/pdf/1702.07995.pdf.

[9] J. Wang, Y. Zheng, Q. Xu, and K. Li, "Data-driven predictive control for connected and autonomous vehicles in mixed traffic," 2021.

[10] M. D. Simoni and C. G. Claudel, "A fast simulation algorithm for multiple moving bottlenecks and applications in urban freight traffic management," *Transportation Research Part B: Methodological*, vol. 104, pp. 238–255, 2017. [Online]. Available: https://www.sciencedirect.com/science/article/pii/S0191261517300802

[11] M. J. Lighthill and G. B. Whitham, "On kinematic waves. II. A theory of traffic flow on long crowded roads," *Prc. Roy. Soc. London Ser A*, vol. 229, pp. 317–346, 1955.

[12] P. Richards, "Shockwaves on the highway," *Operations Research*, vol. 4, pp. 42–51, 1956.

[13] H. Greenberg, "An analysis of traffic flow," *Operations Research*, vol. 7, no. 1, pp. 79–85, 1959. [Online]. Available: http://www.jstor.org/stable/167595

[14] R. T. Underwood, "Speed, volume and density relationships," *Quality and theory of traffic flow*, 1961.

[15] B. Greenshields, J. Bibbins, W. Channing, and H. Miller, "A study of traffic capacity," in *Highway research board proceedings*, vol. 1935. National Research Council (USA), Highway Research Board, 1935.

[16] L. Leclercq, S. Chanut, and J.-B. Lesort, "Moving bottlenecks in Lighthill-Whitham-Richards model: A unified theory," *Transportation Research Record*, vol. 1883, no. 1, pp. 3–13, 2004. [Online]. Available: https://doi.org/10.3141/1883-01

[17] C. F. Daganzo and J. A. Laval, "On the numerical treatment of moving bottlenecks," *Transportation Research Part B: Methodological*, vol. 39, no. 1, pp. 31–46, 2005. [Online]. Available: https://www.sciencedirect.com/science/article/pii/S0191261504000190

[18] C. G. Claudel and A. M. Bayen, "Lax–Hopf Based Incorporation of Internal Boundary Conditions Into Hamilton-Jacobi Equation. Part II: Computational Methods," *IEEE Transactions on Automatic Control*, vol. 55, no. 5, pp. 1158–1174, 2010.

[19] C. Lattanzio, A. Maurizi, and B. Piccoli, "Moving bottlenecks in car traffic flow: a PDE-ODE coupled model," *SIAM J. Math. Anal.*, vol. 43, no. 1, pp. 50–67, 2011. [Online]. Available: https://doi.org/10.1137/090767224

[20] R. Borsche, R. M. Colombo, and M. Garavello, "Mixed systems: ODEs - balance laws," *J. Differential Equations*, vol. 252, no. 3, pp. 2311–2338, 2012. [Online]. Available: https://doi.org/10.1016/j.jde.2011.08.051

[21] J. Lebacque, J. Lesort, and F. Giorgi, "Introducing buses into first-order macroscopic traffic flow models," *Transportation Research Record*, vol. 1644, no. 1, pp. 70–79, 1998. [Online]. Available: https://doi.org/10.3141/1644-08

[22] M. L. Delle Monache and P. Goatin, "Scalar conservation laws with moving constraints arising in traffic flow modeling: An existence result," *Journal of Differentials Equations*, vol. 257, pp. 4015–4029, 2014.

[23] M. Garavello, P. Goatin, T. Liard, and B. Piccoli, "A multiscale model for traffic regulation via autonomous vehicles," *J. Differential Equations*, vol. 269, no. 7, pp. 6088–6124, 2020. [Online]. Available: https://doi.org/10.1016/j.jde.2020.04.031

[24] G. Piacentini, P. Goatin, and A. Ferrara, "Traffic control via platoons of intelligent vehicles for saving fuel consumption in freeway systems," *IEEE Control Syst. Lett.*, vol. 5, no. 2, pp. 593–598, 2021.

[25] S. Liu, H. Hellendoorn, and B. De Schutter, "Model predictive control for freeway networks based on multi-class traffic flow and emission models," *IEEE Transactions on Intelligent Transportation Systems*, vol. 18, no. 2, pp. 306–320, Feb. 2017.

[26] C. Chalons, M. L. Delle Monache, and P. Goatin, "A conservative scheme for non-classical solutions to a strongly coupled PDE-ODE problem," *Interfaces and Free Boundaries*, vol. 19, no. 4, pp. 553–570, 2017.

[27] R. Courant, K. Friedrichs, and H. Lewy, "On the partial difference equations of mathematical physics," *IBM journal of Research and Development*, vol. 11, no. 2, pp. 215–234, 1967.

[28] S. Godunov, "A finite difference method for the computation of discontinuous solutions of the equations of fluid dynamics." *Sbornik: Mathematics*, vol. 47, no. 8-9, pp. 357–393, 1959.

[29] C. Daganzo, "The cell transmission model. Part I: A simple dynamic representation of highway traffic. Berkeley, CA: Institute of Transportation Studies," *University of California, Berkeley*, 1993.